

Article



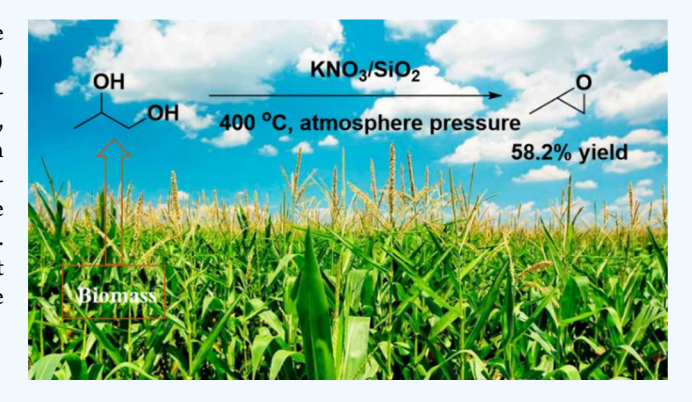
http://pubs.acs.org/journal/acsodf

Catalytic Conversion of Biomass-Derived 1,2-Propanediol to Propylene Oxide over Supported Solid-Base Catalysts

Chengyun Liu, Junna Xin, Jihuai Tan, Tuan Liu, Michael R. Kessler, And Jinwen Zhang Inwen Zhang

Supporting Information

ABSTRACT: A series of supported alkali metal salts were investigated as catalysts to produce propylene oxide (PO) from biomass-derived 1,2-propanediol via dehydrative epoxidation in a solid-gas reaction system. The effects of supports, cations, and anions in the alkali metal salts and calcination temperature were investigated by X-ray diffraction and CO₂temperature-programmed desorption. The results indicate the catalysts with relative mild basicity having higher yields of PO. The highest yield of PO is 58.2% from reactions at 400 °C at an atmospheric pressure over KNO₃/SiO₂. In addition, the catalyst could be reused after calcination in air at 550 °C.



1. INTRODUCTION

Propylene oxide (PO) is an important fine chemical which has been widely used in manufacturing of various products, including polyurethanes, unsaturated resins, and surfactants. Currently, PO is mainly produced from petrochemical propylene via two traditional routes, namely the chlorohydrin and Halcon processes.^{2,3}

In the chlorohydrin process (Scheme 1), propylene is first reacted with a chlorine aqueous solution in which HCl and HOCl are in equilibrium to form a mixture of α - and β chlorohydrin. Then, without intermediate separation, the chlorohydrin is dehydrochlorinated with excess aqueous Ca(OH)₂ to form PO along with byproducts such as dichloropropane and CaCl2.4 Even though the overall selectivity is high (87-90%) by this route, the serious equipment corrosion and environment pollution caused by the byproducts necessitate the search for greener processes.

The Halcon process (Scheme 2) is an indirect oxidation process which normally utilizes tert-butyl or ethylbenzene hydroperoxides as an oxidant to epoxidize propylene. However, byproducts (tert-butanol and acetone from tertbutyl; 1-phenylethanol and acetophenone from ethylbenzene) are also produced during this process.

Recently, to decrease the formation of byproducts during the oxidation process, researchers greatly improved the catalytic performance of titanium silicalite (TS-1) by using novel synthetic technique.⁵ With the help of the TS-1 catalyst, propylene can be converted into PO using H2O2, with H2O as the only significant byproduct in the process. This process has attracted significant attention from the chemical industry because of the environmental benefit. Dow and BASF have announced the construction of the first commercial PO plant using this technology.

However, all of the aforementioned production processes are strongly based on petroleum-derived propylene. Both academia and chemical industry have shown great interests in producing PO from renewable resources. During the last decade, the rapid development of the biomass-based chemical industry offers plenty of chances for people to introduce new production methods from renewable chemical intermediates.⁶ Because PO is a C₃ compound, production of PO from other C₃ structured biomass-derived molecules is reasonable and applicable. In this regard, bio-based 1,2-propanediol (1,2-PDO) is a suitable candidate because the vicinal diols in 1,2-PDO can be converted into epoxide via dehydration. Moreover, 1,2-PDO can be easily obtained from bio-based glycerol and other kinds of C5/C6 sugars via hydrogenolysis, which has already been well-studied and industrialized by BASF, ADM, and S2G companies. The catalytic hydration of 1,2-PDO into PO has received less study and become more difficult because of the high reactivity of PO, which can easily react with coproduced H₂O during the reaction. Fouquet et al.9 claimed a technology for the preparation of PO from 1,2-PDO diesters via pyrolysis reaction. However, the low PO yield (only 15.6%) and severe coking problems hindered the further development of this method. Liu et al. 6,10 reported a method of catalytic transformation of 1,2-PDO into PO using potassium nitrate-loaded silica catalyst. However, the highest yield is only 30.8%, and the detailed relationship between the

Received: May 24, 2018 Accepted: July 30, 2018 Published: August 7, 2018



[†]Composite Materials and Engineering Center, Washington State University, Pullman, Washington 99164-1806, United States

[‡]Department of Mechanical Engineering, North Dakota State University, Fargo, North Dakota 58108, United States

Scheme 1. PO from the Chlorohydrin Process

Scheme 2. PO from the Halcon Process

$$= \underbrace{\begin{array}{ccc} \textit{tert-BuOOH} \\ \text{Cat.} \end{array}} \quad O \underbrace{\begin{array}{cccc} + & \text{BuOH} \end{array}}$$

selectivity of PO and surface properties of the catalyst was not fully studied. Yi et al. 11 studied gas-phase dehydration of 1,2-PDO into PO over Cs/SiO₂ catalyst and illustrated that the strong basic sites formed by Cs⁺ and the interaction between SiO₂ and Cs⁺ dominated the reaction process. Still, the yield for PO needs to be further improved.

To better understand the relationship between the basicity on the surface of catalysts and the selectivity for target product PO, in this work, we systematically studied the effects of support material, cation/anion pair in the alkali metal salt, and calcination temperature on the basicity of the catalyst. Moreover, the stability of catalysts during the reaction process and regeneration process was also studied.

2. RESULTS AND DISCUSSIONS

2.1. Effect of Anion Types of Potassium-Based (K-Based) Salts. Table 1 shows the effects of various anions of K-based salts on the catalytic conversion of 1,2-PDO and selectivity of the products. Compared with other K-based salts, KNO₃/SiO₂ showed the highest activity and selectivity for the target product. The catalytic dehydrative epoxidation of vicinal diols is a base-promoted reaction, ¹¹ and the basicity of catalysts will significantly affect the reaction process. ¹²⁻¹⁵ Therefore, detailed basicity conditions on the surface for each catalyst used in Table 1 were investigated by CO₂-temperature-programmed desorption (TPD) method, and the results are shown in Figure 1 and Table 2.

Theoretically, the surface electronic properties of the SiO₂-supported catalysts are influenced by the anion types. As shown in Figure 1, K₃PO₄/SiO₂ exhibited CO₂-desorption peaks at lower temperatures (<110 °C), which indicated the weak basic sites on the surfaces of these catalysts compared with KNO₃/SiO₂. KNO₂/SiO₂ and K₂CO₃/SiO₂, besides having similar CO₂-desorption peaks around 110 °C, showed desorption peaks in the range of 160–220 °C corresponding to the much stronger basic sites on their surfaces compared with KNO₃/SiO₂. Also, from the perspective of basic sites on the surface of catalysts, although the KNO₃/SiO₂ did not hold the highest basic sites compared with other candidates, both the reaction rate and the selectivity were much better. Because the basicity of catalyst is the key factor for base-promoted reactions, the basicity of catalyst affects the reaction rate and

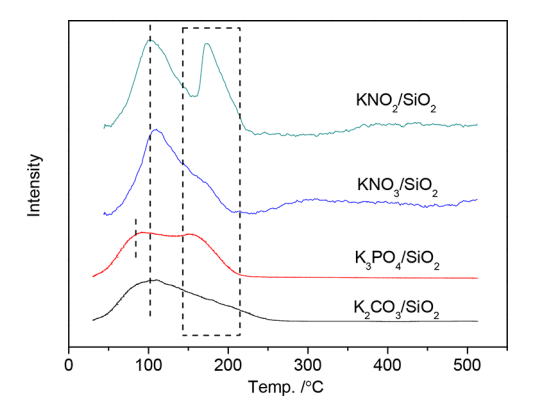


Figure 1. CO₂-TPD profiles of K-based alkali salts supported on SiO₂.

Table 2. Amount of Base Sites on the Surface of Catalysts

catalysts	basic sites ($\times 10^{-5}$ mol/g)
KNO ₂ /SiO ₂	6.18
KNO ₃ /SiO ₂	4.75
K_3PO_4/SiO_2	2.56
K ₂ CO ₃ /SiO ₂	3.03

reaction selectivity significantly. Taking both the reaction results and the basicity of K-based catalysts into consideration, neither the weaker nor stronger basicity generated by the anions other than NO_3^{-1} favors the production of PO. The reaction occurred effectively only under the moderate basicity generated from NO_3^{-1} .

2.2. Catalytic Effects of Different Metal Ions of Alkali Nitrate Catalysts. Table 3 shows the catalytic effects of different alkali nitrates on 1,2-PDO conversion. KNO₃/SiO₂ appears the best candidate for this reaction in terms of conversion of 1,2-PDO and selectivity of PO. To better understand the relationship between surficial basicity and reaction performance, the CO₂-TPD profiles of these SiO₂-supported alkali nitrate catalysts were further studied (Figure 2 and Table 4).

It is obvious that the base strength of SiO₂-supported alkali nitrate catalysts increased with the increase of molecular weight of metal cations from LiNO₃ to CsNO₃, whereas the basic sites reached the maximum in the case of KNO₃/SiO₂ which possibly because of the large radius of Cs⁺ affected the dispersion of CsNO₃ on the surface of SiO₂. Because the reaction rate significantly relied on the surface basicity of catalysts, the conversion of 1,2-PDO increased along with the increase of basicity. On the contrary, even though the basicity

Table 1. Effect of Anion Types in Alkali Catalysts on Catalytic Conversion of 1,2-PDO^a

			Sel. %						
catalysts	conv. %	PO	propionaldehyde	acetone	allyl alcohol	acetol	others		
KNO ₃ /SiO ₂	71.1	81.9	6.9	6.2	3.6	1.4	2.6		
K ₃ PO ₄ /SiO ₂	2.2	13.0	20.7	35.3	20.8	7.5	2.7		
K ₂ CO ₃ /SiO ₂	4.3	20.3	25.9	26.3	9.4	8.8	9.3		
KNO ₂ /SiO ₂	22.4	36.7	14.3	16.6	6.1	20.2	6.1		

[&]quot;Reaction conditions: 400 °C; 1 atm; N2 space velocity: 15 min⁻¹; 1,2-PDO injection rate: 3.6 mL/h; and reaction time: 1 h.

Table 3. Effects of Cations in Alkali Nitrates on Catalytic Conversion of 1,2-PDO^a

		Sel. %					
catalysts	conv. %	PO	propionaldehyde	acetone	allyl alcohol	acetol	others
LiNO ₃ /SiO ₂	11.4	53.8	16.9	16.2	3.6	6.4	3.1
NaNO ₃ /SiO ₂	51.4	60.2	14.7	13.3	4.8	4.5	2.5
KNO ₃ /SiO ₂	71.1	81.9	6.9	6.2	3.6	1.4	2.6
CsNO ₃ /SiO ₂	31.7	78.2	6.2	7.4	4.5	2.7	1.0

"Reaction conditions: 400 °C; 1 atm; N₂ space velocity: 15 min⁻¹; 1,2-PDO injection rate: 3.6 mL/h; and reaction time: 1 h.

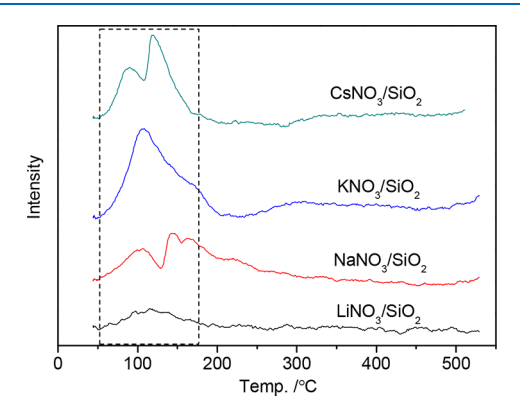


Figure 2. CO_2 -TPD profiles of different alkali nitrates on the surface of SiO_2 .

Table 4. Amount of Base Sites on the Surface of Catalysts

catalysts	basic sites ($\times 10^{-5}$ mol/g)
LiNO ₃ /SiO ₂	2.01
NaNO ₃ /SiO ₂	3.69
KNO ₃ /SiO ₂	6.18
CsNO ₃ /SiO ₂	5.47

of CsNO₃/SiO₂ was stronger than KNO₃/SiO₂, the server coking on the surface of CsNO₃/SiO₂ depressed the conversion of 1,2-PDO during the reaction process (the image of coked catalyst is shown in Figure S12).

2.3. Influence of Support Type. Besides the nature of the cation and anion of the alkali metal salt catalysts, the properties of supports also played critical roles during the reaction process. In Table 5, it is noted that the acidic/basic properties of the supports greatly affected the reaction rate and selectivity. To clarify the influence of support material, the bare supports were tested under the reaction conditions. The results indicated that the supports alone did not promote the formation of PO. Instead, the formations of acetol and allyl alcohol were more favorable in the presence of CaO and MgO,

whereas in the case of γ -Al₂O₃, propional dehyde and acetone were the main products. In the case of SiO₂, the conversion of 1,2-PDO was only 1.8%. This is probably because of the neutral property of SiO₂ because dehydration of 1,2-PDO is a typical kind of acid—base-promoted reaction. KNO₃/SiO₂ exhibited the highest selectivity for producing PO, indicating that KNO₃ is the primary component in catalyzing the formation of PO. In other cases, the KNO₃ only slightly altered the reaction direction and support surface properties still dominated the reaction process. Taking both reactivity and selectivity into consideration, the neutral SiO₂ is the best support for this reaction.

2.4. Effect of Calcination Temperature. The effect of calcination temperature during the catalyst preparation was investigated, and the results are listed in Table 6. In Table 6, it is clear that the calcination temperature greatly influenced both the reaction activity and the selectivity toward PO. The conversion of 1,2-PDO and selectivity for PO increased with increasing calcination temperature from 400 to 550 °C. When calcination temperature reached to 600 °C, the conversion of 1,2-PDO decreased dramatically to 37.0% and the selectivity for PO rolled back to 60.4%. To better understand this phenomenon, several characterization methods such as X-ray diffraction (XRD), N₂ adsorption-desorption analysis, thermogravimetric analysis (TGA), and CO2-TPD were used to identify changes of physical structure, thermal stability, and surface properties of KNO₃/SiO₂ under different calcination temperatures.

In Figure 3, the XRD patterns of KNO₃ were largely retained when the calcination temperature changed from 400 to 550 °C. However, when calcination temperature exceed 600 °C, the characteristic peaks of KNO₃ disappeared completely. This indicated both of the crystal structure, and the physical properties of KNO₃/SiO₂ were strongly related to the calcination process. In Figure 4, the TGA curve of KNO₃/SiO₂ indicated that the supported KNO₃ started to decompose when the calcination temperature was over 400 °C and greatly decomposed at around 560 °C which is in accordance with the

Table 5. Influence of the Support Material on Catalytic Effects of KNO₃

		Sel. %						
catalysts	conv. %	PO	propionaldehyde	acetone	allyl alcohol	acetol	others	
SiO ₂	1.8	0	51.3	8.1	7.3	0	33.3	
CaO	47.5	0	0	34.2	8.9	16.8	40.1	
MgO	12.6	3.4	4.2	5.3	1.2	77.2	8.7	
γ -Al ₂ O ₃	96.3	0	82.1	10.6	4.7	1.3	1.3	
KNO ₃ /SiO ₂	71.1	81.9	6.9	6.2	3.6	1.4	2.6	
KNO ₃ /CaO	69.4	0	0	32.3	7.5	15.6	44.6	
KNO ₃ /MgO	21.3	8.7	9.3	11.2	2.8	63.7	4.3	
KNO_3/γ - Al_2O_3	87.2	0	72.3	20.6	7.1	0	0	

[&]quot;Reaction conditions: temp: 400 °C; pressure: 1 atm; N₂ space velocity: 15 min⁻¹; 1,2-PDO injection rate: 3.6 mL/h; and reaction time: 1 h.

Table 6. Effect of Calcination Temperature of KNO₃/SiO₃ on the 1,2-PDO Conversion^a

		Sel. %					
calcination temperature ($^{\circ}$ C)	conv. %	PO	propionaldehyde	acetone	allyl alcohol	acetol	others
400	56.0	58.8	15.9	12.7	5.6	3.1	3.9
450	64.0	52.3	17.6	15.3	5.9	4.7	4.2
500	67.3	64.7	10.8	12.3	4.5	4.2	3.5
550	71.1	81.9	6.9	6.2	3.6	1.4	2.6
600	37.0	60.4	12.4	7.9	6.2	3.8	9.3

[&]quot;Reaction conditions: 400 °C; 1 atm; N₂ space velocity: 15 min⁻¹; 1,2-PDO injection rate: 3.6 mL/h; and reaction time: 1 h.

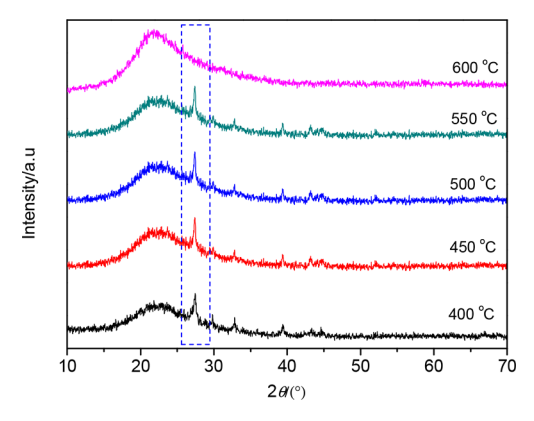


Figure 3. XRD patterns of KNO_3/SiO_2 under different calcination temperatures.

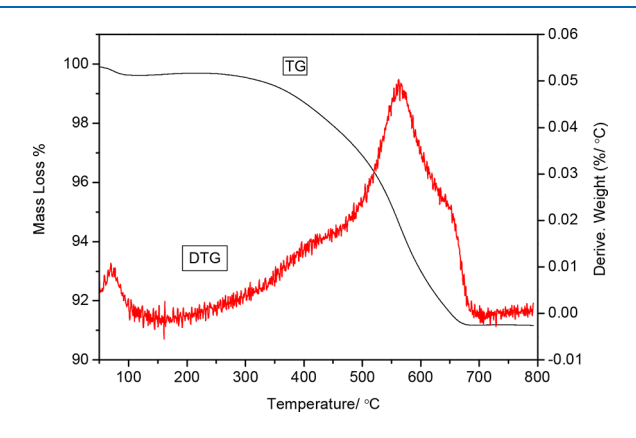


Figure 4. TGA of KNO₃/SiO₂.

change of XRD patterns. Because the decomposition of supported KNO $_3$ will certainly affect the porous structure of catalysts and its corresponding catalytic performance, the N $_2$ adsorption—desorption analysis was carried out and the results were shown in Table 7. In Table 7, with the increase of calcination temperature, both the surface area and the pore volume decreased which means the supported KNO $_3$ nanocrystals would aggregate and block the pores within SiO $_2$.

Table 7. Surface Area and Pore Volume of Catalysts under Different Calcination Temperatures

calcination temperature ($^{\circ}$ C)	BET $\left(m^2/g\right)$	pore volume (cm ³ /g)
400	201.2207	0.520720
450	195.4656	0.523864
500	171.5172	0.506030
550	40.5168	0.064598
600	31.4878	0.040925

Additionally, because of the heterogeneous reaction always happening on the surface of catalyst, the surface properties are crucial for the overall reaction trend. The $\rm CO_2\text{-}TPD$ profiles (Figure 5 and Table 8) further illustrated the change of surface basic property of $\rm KNO_3/SiO_2$ under different calcination temperatures.

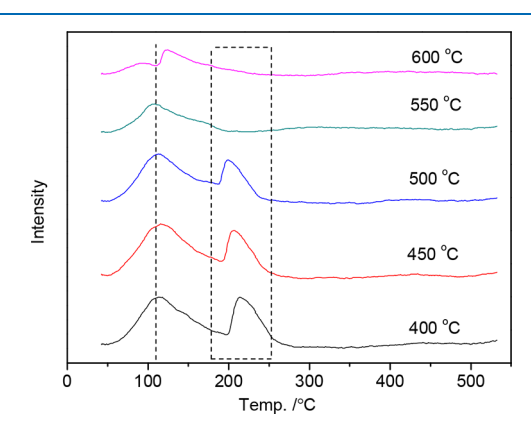


Figure 5. CO_2 -TPD profiles of KNO_3/SiO_2 under different calcination temperatures.

Table 8. Amount of Base Sites on the Surface of Catalysts

calcination temperature ($^{\circ}$ C)	basic Sites ($\times 10^{-5}$ mol/g)
400	9.16
450	9.08
500	8.72
550	6.18
600	4.23

In Figure 5, the KNO₃/SiO₂ calcinated between 400 and 500 °C exhibited similar desorption peaks, which remained almost unchanged. Although the catalyst calcinated at 550 °C or higher temperatures, the desorption peaks at the lower temperature red-shifted and the desorption peaks at 225 °C disappeared. On the other hand, although the total basic sites on the surface of KNO₃/SiO₂ decreased along with the increase of calcination temperature (Table 8), the KNO₃/SiO₂ prepared at 550 °C still exhibited the highest conversion and selectivity of PO. Because the intensity and position of CO₂ desorption peaks are strongly related to the surface basic properties, which also dominated the reaction process. This suggests that the weak basic sites corresponding to the CO₂ desorption peak at ~105 °C are more favorable for the formation of PO. The slight change of basicity (CO2desorption peak from 125 to 105 °C) would significantly affect the reaction process and selectivity of the target product.

2.5. Effect of Reaction Temperature. In Table 9, the reactivity and selectivity for PO increased with a reaction

Table 9. Effect of Reaction Temperatures^a

			Sel. %					
catalysts	temp (°C)	conv. %	PO	propionaldehyde	acetone	allyl alcohol	acetol	others
KNO ₃ /SiO ₂	300	0	0	0	0	0	0	0
KNO ₃ /SiO ₂	350	3.7	56.2	17.3	10.9	5.8	4.7	5.1
KNO ₃ /SiO ₂	400	71.1	81.9	6.9	6.2	3.6	1.4	2.6
^b KNO ₃ /SiO ₂	400	18.7	59.1	14.2	15.3	4.2	3.8	3.4
KNO ₃ /SiO ₂	450	61.1	54.7	16.8	11.6	5.6	4.4	6.9
KNO_3/SiO_2-10 wt % H_2O	400	0	0	0	0	0	0	0

[&]quot;Reaction conditions: 400 °C; 1 atm; N₂ space velocity: 15 min⁻¹; and 1,2-PDO injection rate: 3.6 mL/h. bReaction time: 1 h.

temperature up to 400 °C, and then it started to decrease when the reaction temperature is increased to 450 °C. When the reaction time was extended to 2 h at 400 °C, both the reactivity and the selectivity for PO sharply dropped because of coking on the surface of the catalyst. To solve this problem, we tried to introduce 10 wt % water vapor into the reaction system, as shown in Table 9. However, there was no PO formed under that circumstance, probably because of the higher reactivity of the produced PO reacting with water under such harsh reaction conditions.

Further investigation of the coking problem on the surface of coked catalyst was performed by TGA. In Figure 6, there are

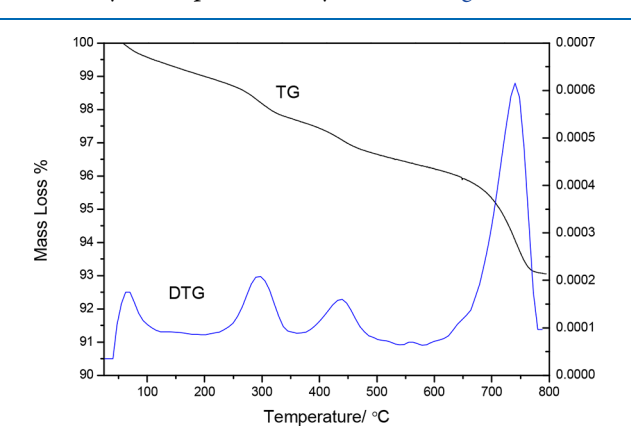


Figure 6. TGA of catalyst after 2 h reaction.

four main peaks in the differential thermogravimetry curve of a coked catalyst. Because the decomposition temperature of KNO $_3$ is around 550 °C, 16 the peaks below 500 °C are likely because of the decomposition of the coked substrate. This means the coked catalysts can be regenerated at 500 °C under air atmosphere. The catalytic performance of the regenerated catalyst is shown in Table 10.

In Table 10, it is noted that after three times recycling, the catalytic activity of catalyst and the selectivity for PO exhibited some moderate decreases, but the latter still remained at a relatively high level. Therefore, this catalytic process could be

more practical by coupling with a regeneration system which maintains the reaction processing continuously.

3. CONCLUSIONS

In this article, a novel catalytic system for producing PO from bio-based 1,2-PDO has been investigated. Several types of alkali metal salt catalysts were evaluated. Support type, cation/anion pair in the alkali metal salt, and calcination temperature greatly affected surface properties of the catalysts, which, in turn, dominated the conversion process and selectivity. The moderate strength of basic sites favored the reaction conversion and selectivity to PO. The highest yield of PO was 58.2% under 400 °C at atmosphere pressure over KNO $_3$ / SiO $_2$, and the catalyst could be reused several times after being calcinated at 500 °C with air.

4. EXPERIMENTAL SECTION

4.1. Preparation of Supported Alkali Metal Catalysts.

The supported alkali metal catalysts were prepared by the impregnation method. Typically, the porous support was impregnated in a nitrate solution of alkali metal (alkali metal = Li, Na, K, or Cs) at ambient temperature while stirring for 4 h. After that, the resulting precursor of the supported catalyst was dried at 120 °C overnight and then calcinated at 550 °C for 6 h. The supporting ratio of alkali metal on the surface of support is 1.5 mmol/g.

4.2. Reactivity Tests. A fixed-bed quartz reactor was used to evaluate the catalytic performance of the catalyst for the dehydration of 1,2-PDO into PO. Temperature was measured by a K-type thermocouple and was controlled with an external electrical furnace. The reaction was performed using a 0.3 g of catalyst sample diluted with SiC (1:1 mass ratio) which greatly disperses the reaction heating. 1,2-PDO was injected at a rate of 3.6 mL/h into a preheating zone which was maintained at 473 K and connected to the top of the reactor at a N₂ space velocity of 15 min⁻¹. The product was collected hourly, and acetonitrile was used as an external standard for quantification.

The products were analyzed using a gas chromatography (GC)/GC-mass spectrometry (MS) (Agilent 6890) equipped with a flame ionization detector and DB-WAX capillary

Table 10. Catalytic Performance of Regenerated Catalysts^a

		Sel. %							
1	0/								
recycle times	conv. %	PO	propionaldehyde	acetone	allyl alcohol	acetol	others		
1	50.5	78.3	8.5	5.4	2.6	1.1	4.1		
2	46.7	70.3	9.6	7.3	4.9	2.7	5.2		
3	40.8	68.3	12.8	10.3	4.5	3.2	0.9		

[&]quot;Reaction conditions: 400 °C; 1 atm; N_2 space velocity: 15 min⁻¹; 1,2-PDO injection rate: 3.6 mL/h; and regeneration conditions: calcinated in air atmosphere at 500 °C.

column, and the oven temperature ramp was set at 333 K for 2 min and then increased to 553 K at a rate of 10 K/min. The data acquired at 1 h of the reaction time were used to compare the catalytic activity of the catalysts. All of the experimental data were the average values for three times experimental runs.

4.3. Characterization of Catalysts. The XRD patterns were measured by a Rigaku D-max 2500-PC powder X-ray diffractometer with Cu K α radiation (1.5406 Å) in an operating mode of 50 kV and 100 mA.

TPD of CO₂ was carried out using Micromeritics AutoChem II chemisorption analyzer. Prior to the analysis, 0.2 g of sample was heated at 673 K for 1 h under a He flow to remove adsorbed impurities. After cooling to 323 K, the sample was saturated with a probe gas by a flow of 10.2% CO₂/He. The physisorbed probe gas was removed by flushing of He flow at 373 K. After the sample was cooled to 323 K and the thermal conductivity detector signal was stabilized, the signal was recorded with increasing temperature from 323 to 823 K at a rate of 10 K/min under the flow of He.

Thermal stability was measured using a thermogravimetric analyzer, and the sample (\sim 10 mg) was scanned from 50 to 800 °C at a heating rate of 10 K/min under nitrogen or oxygen atmosphere.

 $\rm N_2$ adsorption—desorption analysis was carried out using a Micromeritics ASAP-2010 instrument. The total surface area of the samples was calculated by the Brunauer—Emmett—Teller (BET) method ($P/P_0=0.1-0.2$). The pore volume and pore size distributions were obtained from the desorption branches of the isotherms using Barrett—Joyner—Halenda methods.

ASSOCIATED CONTENT

S Supporting Information

The Supporting Information is available free of charge on the ACS Publications website at DOI: 10.1021/acsomega.8b01121.

GC–MS spectrum of 1,2-PDO reaction products; mass spectrum of PO; mass spectrum of propionaldehyde; mass spectrum of acetone; mass spectrum of 2-ethyl-4-methyl-1,3-dioxolane; mass spectrum of 1-propanol; mass spectrum of allyl alcohol; mass spectrum of (E)-2-methylpent-2-enal; mass spectrum of 1-hydroxypropan-2-one; mass spectrum of 3-methylcyclopent-2-en-1-one; mass spectrum of 1,2-PDO; and images of CsNO₃/SiO₂ catalyst before and after reaction (PDF)

AUTHOR INFORMATION

Corresponding Authors

*E-mail: junna.xin@wsu.edu (J.X.).

*E-mail: jwzhang@wsu.edu (J.Z.).

ORCID 6

Junna Xin: 0000-0001-6373-937X Tuan Liu: 0000-0001-7868-9424

Michael R. Kessler: 0000-0001-8436-3447 Jinwen Zhang: 0000-0001-8828-114X

Notes

The authors declare no competing financial interest.

■ ACKNOWLEDGMENTS

The authors are grateful for financial support from the Joint Center for Aerospace Technology Innovation (JCATI 2015-2016).

REFERENCES

- (1) Tullo, A. H.; Short, P. L. Propylene Oxide Routes Take Off. Chem. Eng. News 2006, 84, 22-23.
- (2) Trent, D. L. Kirk-Othmer Encyclopedia of Chemical Technology, 4th ed.; Wiley: New York, 1996; pp 271–278.
- (3) Wegener, G.; Brandt, M.; Duda, L.; Hofmann, J.; Klesczewski, B.; Koch, D.; Kumpf, R.-J.; Orzesek, H.; Pirkl, H.-G.; Six, C.; Steinlein, C.; Weisbeck, M. Trends in industrial catalysis in the polyurethane industry. *Appl. Catal., A* **2001**, *221*, 303–335.
- (4) Weissermel, K.; Arpe, H.-J. *Industrial Organic Chemistry*, 2nd ed.; VCH Verlagsgesellschaft, 1993; pp 268–312.
- (5) Zuo, Y.; Wang, X.; Guo, X. Synthesis of titanium silicalite-1 with small crystal size by using mother liquid of titanium silicalite-1 as seed. *Ind. Eng. Chem. Res.* **2011**, *50*, 8485–8491.
- (6) Corma, A.; Iborra, S.; Velty, A. Chemical Routes for the Transformation of Biomass into Chemicals. *Chem. Rev.* **2007**, *107*, 2411–2502.
- (7) Dasari, M. A.; Kiatsimkul, P.-P.; Sutterlin, W. R.; Suppes, G. J. Low-pressure hydrogenolysis of glycerol to propylene glycol. *Appl. Catal., A* **2005**, *281*, 225–231.
- (8) Yu, Z.; Xu, L.; Wang, Y.; et al. A new route for the synthesis of propylene oxide from bio-glycerol derivated propylene glycol. *Chem. Commun.* **2009**, *26*, 3934–3936.
- (9) Fouquet, G.; Merger, F.; Baer, K. Verfahren zur herstellung von propylenoxid. Germany Patent DE 2709440 A1, 1978.
- (10) Liu, Z.; et al. Catalyst used in preparation of propylene epoxide by utilizing 1,2-propylene glycol gas dehydration and application. Chinese Patent CN 101773822 A, 2010.
- (11) Kim, T. Y.; Baek, J.; Song, C. K.; Yun, Y. S.; Park, D. S.; Kim, W.; Han, J. W.; Yi, J. Gas-phase dehydration of vicinal diols to epoxides: Dehydrative epoxidation over a Cs/SiO₂ catalyst. *J. Catal.* **2015**, 323, 85–99.
- (12) Shi, B. C.; Davis, B. H. Alcohol Dehydration: Mechanism of Ether Formation Using an Alumina Catalyst. *J. Catal.* **1995**, *157*, 359–367.
- (13) Calvino-Casilda, V.; Martin-Aranda, R.; Sobczak, I.; Ziolek, M. Modification of acid—base properties of alkali metals containing catalysts by the application of various supports. *Appl. Catal., A* **2006**, 303, 121–130.
- (14) Delsarte, S.; Florea, M.; Maugé, F.; Grange, P. Understanding the role of nitridation in butan-1-ol and butan-2-ol dehydration mechanisms over oxynitrides. *Catal. Today* **2006**, *116*, 216–225.
- (15) Delsarte, S.; Grange, P. Butan-1-ol and butan-2-ol dehydration on nitrided aluminophosphates: influence of nitridation on reaction pathways. *Appl. Catal., A* **2004**, *259*, 269–279.
- (16) Freeman, E. S. The Kinetics of the Thermal Decomposition of Potassium Nitrate and of the Reaction between Potassium Nitrite and Oxygen. J. Am. Chem. Soc. 1957, 79, 838–842.